

Title	Automatic UAV surface inspection method for underground infrastructure - a case study of Dublin Port Tunnel
Authors	Zhang, Ran;Li, Zili
Publication date	2023
Original Citation	Zhang, R. and Li, Z. (2023) 'Automatic UAV surface inspection method for underground infrastructure - a case study of Dublin Port Tunnel', Proceedings of the 11th International Conference on Sustainable Development in Building and Environment (SuDBE2023), Aalto, Finland, 14-18 August, Extended Abstract 288 (9pp).
Type of publication	Conference item
Rights	© 2023, the Authors.
Download date	2024-05-21 00:41:42
Item downloaded from	https://hdl.handle.net/10468/15788

Citation:

Zhang R. and Li Z. (2023) Automatic UAV surface inspection method for underground infrastructure – a case study of Dublin Port Tunnel. In: *Proceedings of International Conference on Sustainable Development in Building and Environment - SuDBE 2023*, Aalto, Finland, 14th August– 18th August 2023. Extended Abstract #288. 9 pp.

Conference topic:**Automatic UAV surface inspection method for underground infrastructure – a case study of Dublin Port Tunnel**

Ran Zhang¹ Zili Li^{1,2} *

¹ Discipline of Civil, Structural and Environmental Engineering, School of Engineering and Architecture, University College Cork, T12 K8AF Cork, Ireland

² Science Foundation Ireland, Irish Centre for Applied Geoscience (iCrag), D04 V1W8 Dublin, Ireland

*Corresponding email: zili.li@ucc.ie

ABSTRACT

This paper proposes an automatic data acquisition method for automated UAV inspection in a complex underground road tunnel without a global navigation satellite system (GNSS) signal. The gathered image data is then processed to create a 3D reconstruction of the road tunnel for structural condition assessment.

KEYWORDS Road tunnels, Surface inspection, Unmanned aerial vehicles, Navigation

1. INTRODUCTION

Regular structural inspection of the tunnel surface is essential for asset maintenance and relevant repair to ensure the infrastructure's safety and serviceability. In general, the surface health inspection of the tunnel includes surface cracks, spalling, water leakage, and blockages in drainage pipes (BOULOGNE et al. 2015). Dublin Port Tunnel (DPT) is one of the longest urban road tunnels in Europe. The DPT structure comprises some complex sections, including a shaft, lay-by tunnel, and cross-passage-connected twin tunnel, where a series of surface defects have been developing over the years, necessitating regular structural health assessment. However, manual inspections of highway tunnels are subjective and costly. The use of automated robots can facilitate the inspection of large-scale geotechnical assets (Montero et al. 2015). The robotic approach enables the automatic identification of structural damage and enhances digital infrastructure asset management. It offers the advantage of low-cost image data acquisition and adaptability to different types of geotechnical assets, such as shafts, tunnels, and pipelines.

However, automatic inspection faces challenges in road tunnels, including a lack of GNSS signals, low light, and complex geometric conditions, especially in precise UAV positioning and data acquisition. For example, at the DPT tunnel, the twin tunnel has a cross passage in the middle and laybys for cars, which complicates the route planning for automatic inspection. In addition, DPT has many facilities such as signals, signage, fire hydrants, wall-mounted loudspeakers, etc. These factors limit data collection by ground vehicles or rail cars, while UAVs can adapt to such a complex environment and collect data on the tunnel's facilities from multiple angles.

Previous studies usually utilized additional sensors or markers, such as using LiDAR or artificial landmarks to aid in the autonomous positioning of UAVs. However, active positioning modules and machine vision-assisted visual positioning rely on excessively high battery consumption and computational power. Therefore, most of their drones have a rather short endurance of around 15 minutes (Tan et al. 2018), making it not practical for use in confined environments by micro UAVs with limited computing power and power supply. Furthermore, these previous automated UAV

studies were usually only able to use simple linear trajectories to fly at constant velocity in shafts. That is, data acquisition with a 360° camera in one-dimensional motion can only be adapted to a smaller number of inspection scenarios but fails to accommodate the complexity of the structure or overcome motion blur.

In this study, an automatic inspection method move-pause-photo (MPP) is designed to enable adaptive navigation and automatic acquisition in 3D space. It utilizes visual distance sensing and reactive algorithms for navigation in road tunnels. Data acquisition in a field of vision (FoV) of (-90°, 70°) is through gimbal rotation, over the discrete movement of the UAV along the tunnel axis.

After that, the developed novel UAV data acquisition method is applied to Dublin Port Tunnel as shown in Figure 1. The UAV platform is a commercial version of DJI Mavic 2 Enterprise dual (M2ED) and the associated UAV navigation control method is built into a Mobile software development kit (MSDK). An external light module of M2ED is available to ensure high-quality visual data. The algorithm adjusts the navigation strategy based on the real-time data gathered by the sensors. This method enables automated surface data acquisition and maintenance analysis in road tunnels with complex geometry, uneven illumination, and a lack of GNSS signal.

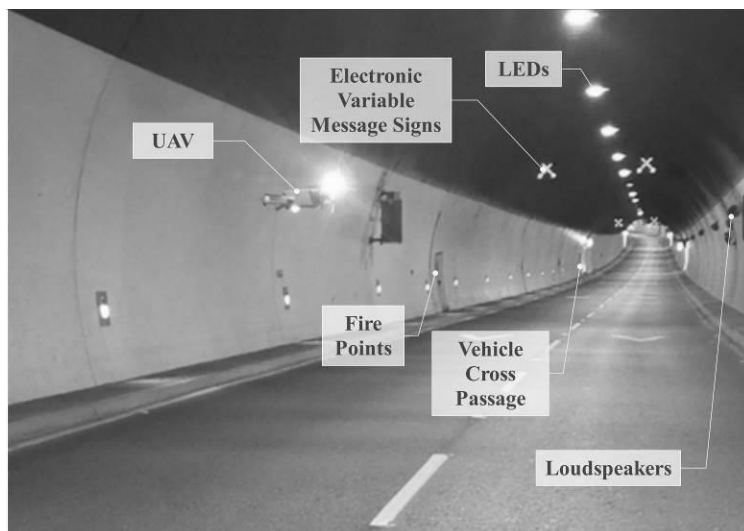


Figure 1 Automatic UAV inspection in DPT road tunnel

2. IMAGE DATA COLLECTION BY AUTOMATIC DRONE INSPECTION

2.1 Challenges and Solutions in the Road Tunnel Scanning

The Dublin Port Tunnel is a key transportation infrastructure project between the port and the national road network. Construction of the tunnel commenced in 2001 and was completed in 2006. Overall, the tunnel stretches approximately 4.5 kilometers and the geometry of the critical vehicle cross-passage section for UAV inspection is illustrated in Figure 2 (1).

Firstly, the complexity of the tunnel structure poses a challenge to image acquisition. Compared to conventional ground vehicles, UAVs enable image collection of 3D component information from different angles in DPT. Another challenge is the insufficient light intensity and intensity variance. In general, reliable navigation in a complex tunnel requires sufficient light intensity as much as 15 lux for the UAV visual sensors. Nevertheless, LEDs in DPT provide inconsistent and weak lights, as shown in Figure 2 (2). Therefore, the auxiliary lights module is used in close-range inspection with its maximum luminance of 11 lux at a distance of 30m to the spotlight and its FoV of 17°, as in Figure 2 (3). The enhanced luminance by the auxiliary light module will create 620 lux at most for the UAV visual sensors and satisfactory image quality. Due to the symmetrical nature of the structure, the area boxed in Figure 2 (1) was chosen as the area for UAV inspection, where more cracks are observed than in the opposite symmetrical section.

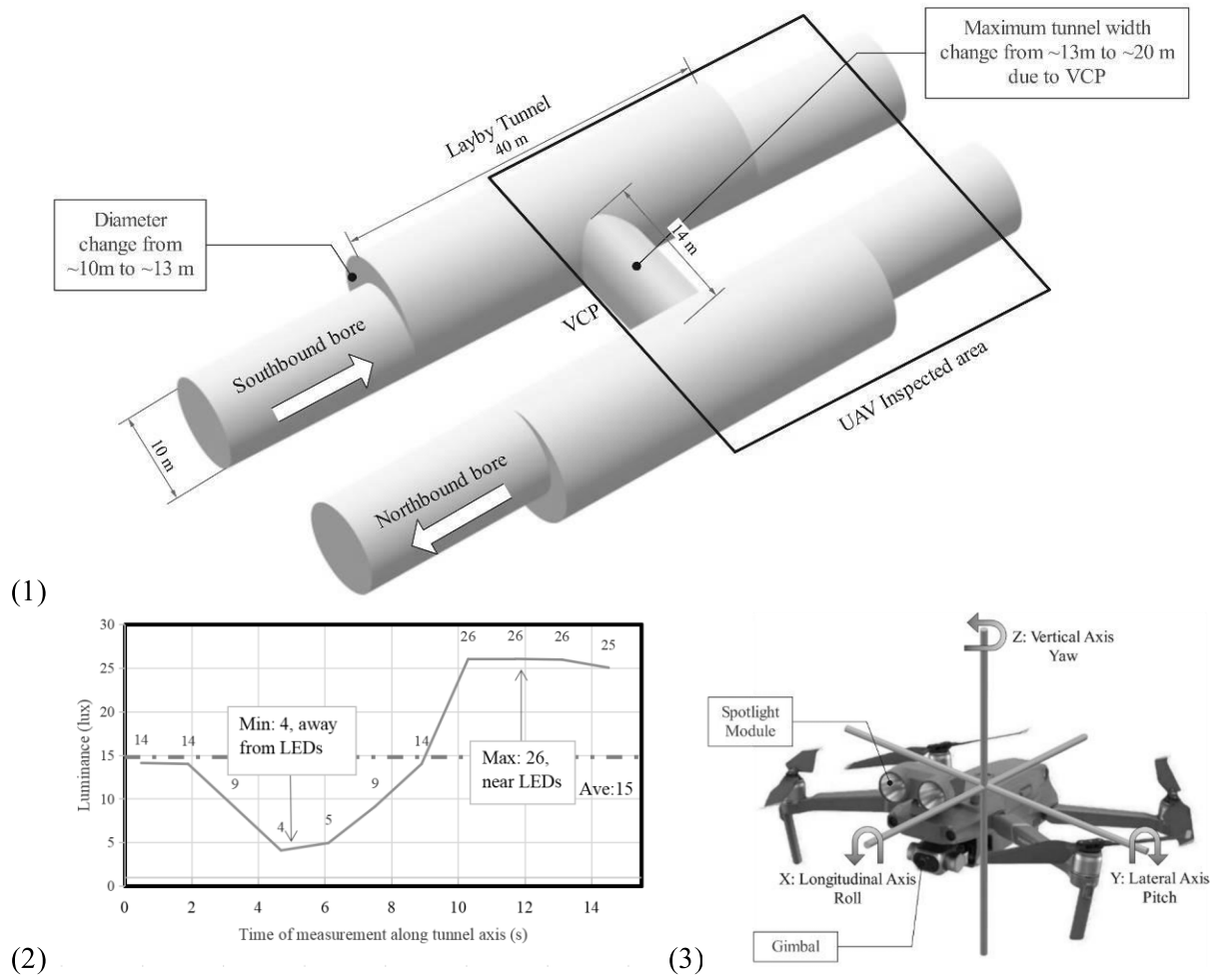


Figure 2 (1) Illustration of cross-passage geometry in the UAV inspected area. (2) Intensity variation of reflective light on tunnel side wall along DPT axis and (3) Spotlights module installed on UAV

Photogrammetry in unmapped tunnels needs to overcome the lack of geometric constraints. A tunnel is a near-barrel 3D structure where slices per unit length can be expanded radially into a 2D rectangular shape, as shown in Figure 3. Then for 2D surface scanning, a grid pattern is commonly used to guarantee sufficient frontal and side overlapping rate (Jiménez-Jiménez et al. 2021). The area of interest is the grey zone in both data acquisition and tunnel. Moreover, for the clarity of the data, motion blur should be avoided, so the MPP method obtains photographs rather than recording videos. As a result, a 3D reconstruction model can be created based on the gathered photos.

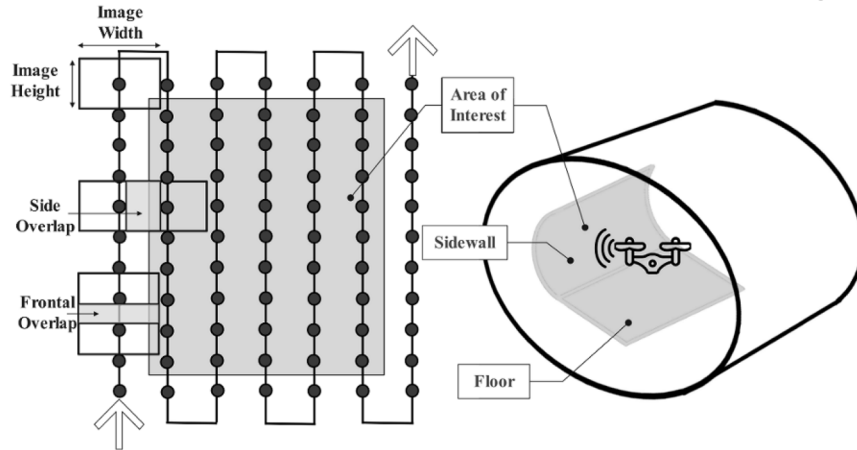


Figure 3. Application of classical grid data acquisition pattern in UAV inspections.

2.2 Data collection methods

The data for this study was collected using the DJI Mavic2 Enterprise Dual (M2ED), a commercial UAV that can mount a spotlight module to provide a complementary forward-looking light source, as shown in Figure 2 (3). The inspection method is developed from the DJI Mobile software development kit (MSDK) for automatic navigation and data acquisition in road tunnels. Each strip in the grid pattern contains UAV around 11 images, to guarantee frontal overlap α larger than 85%. Formula 1 is utilized to determine the number of images, denoted as 'n', to be scanned per strip in the vertical direction. And Formula 2 gives the horizontal panning distance Dh between strips:

$$n \times \theta \geq |Rv|, s.t. \theta \leq FoV \times (1 - \alpha) \quad (1)$$

$$D_h < (1 - \alpha)W, s.t. W = 2D \tan \frac{Fov}{2} \quad (2)$$

Where the FoV of the UAV is 84° . The gimbal rotates in a theoretical range Rv of $(-90^\circ, 30^\circ)$ vertically and Rh $(-75^\circ, 75^\circ)$ horizontally. Referral interval θ is 10° for image capture. The projections of the image center on the inspected surface could be represented by red dots in Figure 3. W is the width of the scene in a single frame. D is a user-defined distance from the lens to the front wall.

The UAV travels inside the tunnel with the body and gimbal aligned to the wall during a surface inspection. The UAV adjusts three flight strategies through reactive control as shown in Table 1 and Figure 4, according to distance data between UAV and the front/back wall. Lateral position is adjusted through real-time feedback control. Yaw control also is through feedback from frontal distance readings in the four sectors. The longitudinal control uses a static passive control predetermined by users. The UAV advances and hovers between the data acquisition spots, as shown in Figure 4 (1b) (2b) (3b). The camera has a 2s shutter interval. The scanning speed is 3m/min in obstacle-free conditions. Since the UAV program allows the user to enter control parameters such as the lateral position to the wall, the flight height, and the step length of panning, it enables adaptive inspection in various 3D environments compared to conventional automatic inspection by ground vehicles.

Table 1 UAV navigation strategy corresponding to real-time UAV measurement of tunnel diameter

Lateral movement strategy	Tunnel's diameter from the sensors' data	Environmental factors for surface inspection
On the tunnel axis	Small diameters (<6m) and small diameter variations	Close-range inspection in a simple environment, favorable for control
Constant distance to the front wall (user-defined)	Large diameters (<20m), or large diameter variations (but still <15% of the diameter)	In large/complex or dim environments, still with known references to move along
No lateral movement	Other situations (e.g. 100m or no update from sensors)	complex or dark environments, with no lateral positioning data

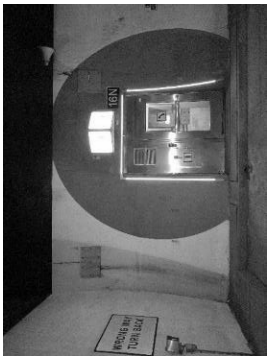
2.3 Standard Operating Procedure (SOP) for image acquisition

A standard operating procedure (SOP) is proposed for drone surface data acquisition of road tunnels. The proposed SOP considers the unfavorable conditions of the DPT road tunnel. In DPT, the problem focuses on tunnel geometry, which is the varying tunnel diameter along the longitudinal direction due to cross passage, layby sections, etc. In the drone inspection field test, UAVs can largely fly automatically with limited manual supervision. Operators' surveillance allows drone inspection in DPT to follow the procedures below:

1. Conduct image acquisition in the proximity of the take-off point.
2. Determine UAV navigation strategy based on environmental conditions.
3. Make lateral adjustments and collect data according to the navigation strategy.
4. Advance the UAV by 1.5m while refining the yaw orientation.
5. Repeat Steps 2-4 for drone inspections at different heights until the inspection area is covered.
6. Replicate the above procedures to inspect the opposing side of the tunnel wall.



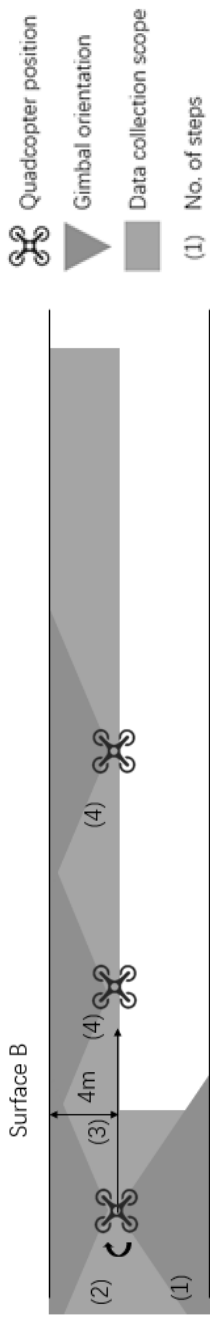
(1a) Scene A: Example of a slightly curved surface



(2a) Scenario B: Example of small tunnel diameter change -- emergency Lay-bys

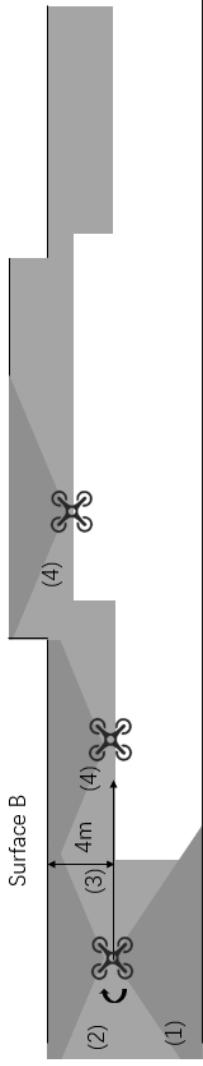


(3a) Scenario C: Example of large tunnel diameter change



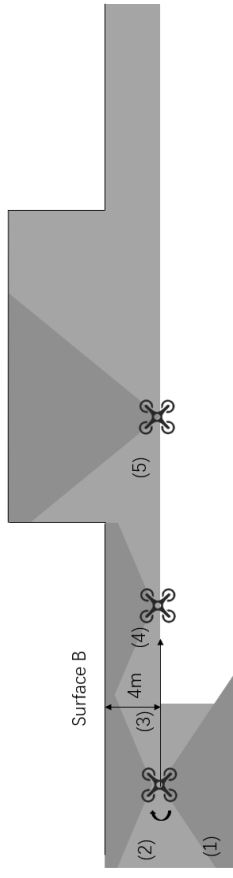
Surface A

(1b) Scenario A: Schematic top view of a simple tunnel surface, smooth, probably with slight diameter change. UAV moves along a straight routine parallel to the tunnel axis.



Surface A

(2b) Scenario B: Schematic top view of tunnel sections with varying complexity, including a simple large-diameter tunnel, a complex section with small diameter change, and/or a tunnel under weak light conditions. UAV moves along the tunnel side wall.



Surface A

(3b) Scenario C: Schematic top view of a complex tunnel section with significant changes in diameter and/or low light conditions. UAV moves along the original route.

Figure 4 Three flying strategies in the MPP method for UAV inspection varying structural and luminance.

3. IMAGE DATA PROCESSING

This automatic UAV inspection gathered a 9.56 GB dataset of 1619 images in total from the Southbound tunnel section over 32m and 38m in the opposite tunnel section at Northbound. The UAV inspection can cover a height of 5.5m out of 6.3 m's total height in DPT, which demonstrates the UAV control accuracy in road tunnel inspection.

The post-processing is conducted through Pix4Dmapper, including dataset management, automatic alignment, image stitching, and point cloud model creation. In post-processing, the tunnel diameter is used as a scale constraint, which solves the problem of scale ambiguity in structure from motion (SFM) reconstruction in a tunnel. The orthomosaics of the four tunnel side walls at the twin tunnels are shown in Figure 5 (a-d), whilst the top views of the two tunnels are shown in Figure 5 (e). All the cracks are marked with red color, spalling in purple circles, and leakage in yellow circles. The regions near the VCP and away from the VCP are marked with blue and red rectangular, respectively.

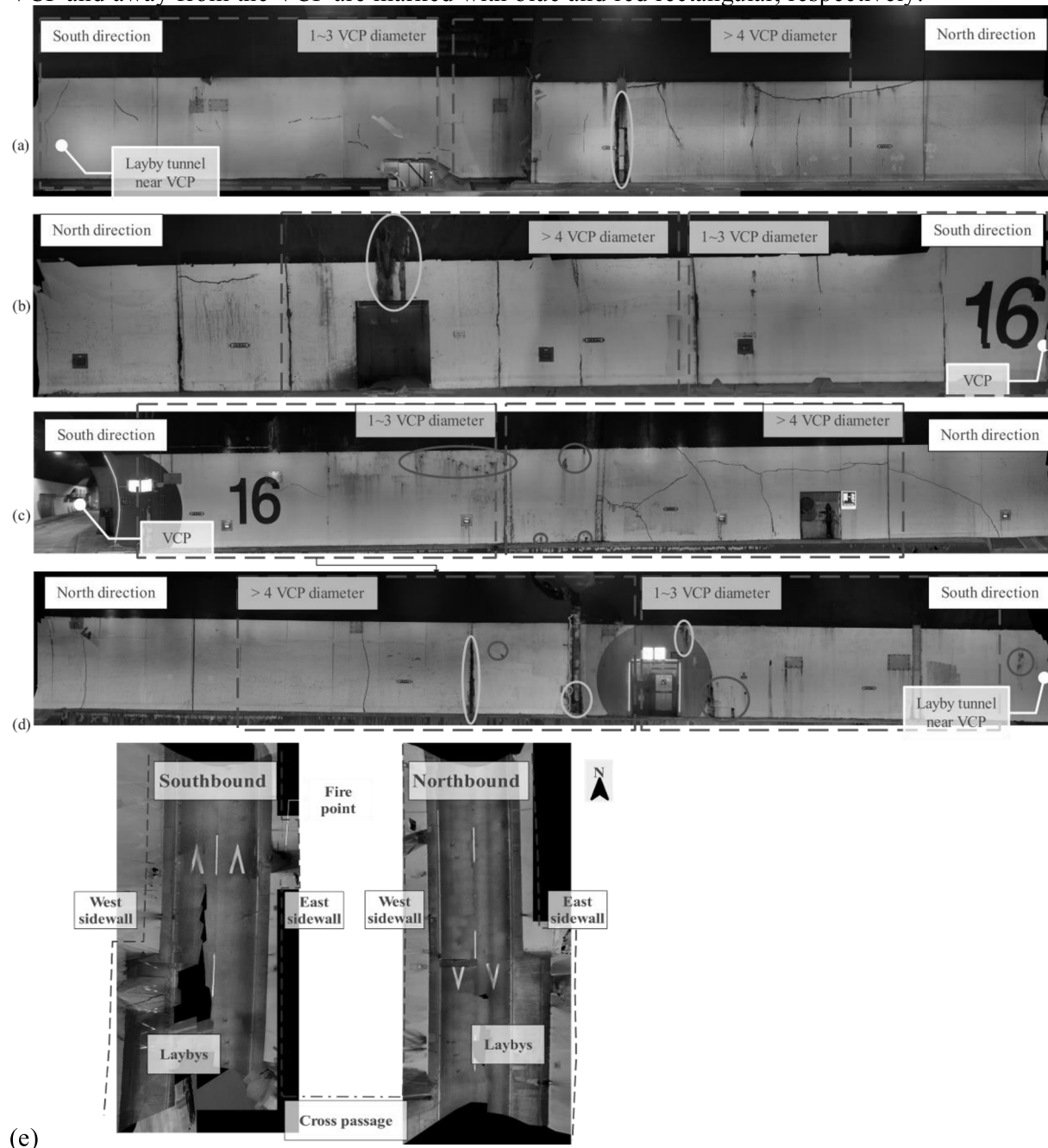
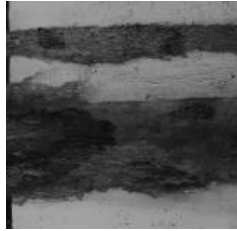
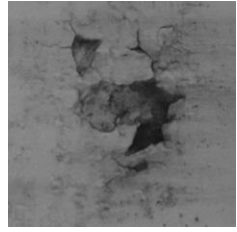

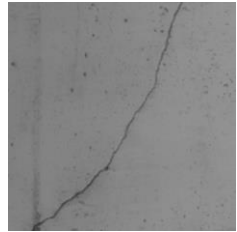
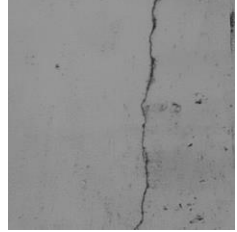


Figure 5. Orthomosaics and crack distribution (marked in red) for four tunnel side walls: (a) southbound west (b) southbound east (c) northbound west (d) northbound east; and (e) the overview

4. TUNNEL CONDITION PRELIMINARY ASSESSMENT

In general, the tunnel structural health condition inspection includes spalling, cracks, and water leakage. The findings about defect distribution and the possible causes are listed in Table 2. In the following part of the analysis, the scale of VCP diameter is adopted to study the impact of VCP on structure health, as major cracks have a length varying from around 0.5 m to 10 m,

Table 2 Defects in DPT

Defect	Water ingress	Spalling due to compressive load	Vertical structural cracks	Diagonal structural cracks	Horizontal structural cracks
Example images in DPT					
Possible causes of defects	<ul style="list-style-type: none"> - Fluctuation or water table flow rate change in the surrounding ground - Water leaks from another network - Loss or absence of the lining's water-tightness - Failure of drains 	<ul style="list-style-type: none"> - Excessive compression in the lining, exceeding the mechanical strength of the concrete 	<ul style="list-style-type: none"> - Deformation or change in thickness of the lining - Shearing of the lining - Differential settlement 	<ul style="list-style-type: none"> - Pathological origin often related to ground movement - Differential settlement - Twisting or oblique shearing of the arch to the axis 	<ul style="list-style-type: none"> - Pathological origin is often related to the deterioration of the lining, which may or may not result from the surrounding ground
Locations (relative to VCP and laybys)	<ul style="list-style-type: none"> - Starting from the black roof mostly. - Along the construction joint also. - Some from the small fissures 	<ul style="list-style-type: none"> - On top of the west northbound sidewall. 	<ul style="list-style-type: none"> - From the crown to the floor, - Both appear on the east and west side 	<ul style="list-style-type: none"> - At various heights - Away from VCP, - Not affected by layby 	<ul style="list-style-type: none"> - Middle of the tunnel side wall, - Away from VCP, - Not affected by layby
Distribution patterns	<ul style="list-style-type: none"> - Major water ingress comes in spaced arrangement from structural joints; - Small water ingress appears in patches under fissures 	<ul style="list-style-type: none"> - Dense near Northbound west sidewall 	<ul style="list-style-type: none"> - Isolated and continuous, across the sidewall 	<ul style="list-style-type: none"> - Cracks in succession, with various lengths of both short and long cracks 	<ul style="list-style-type: none"> - 0.5 per meter, often a long crack
Possible consequences if left unattended	<ul style="list-style-type: none"> - Deterioration of the lining (leaching, erosion) and weakening of the structures - Falling of lining elements 	<ul style="list-style-type: none"> - Further deterioration in the affected area and the severity - Critical phenomenon (even if there is no deformation of the arch in most cases) 	<ul style="list-style-type: none"> - Weakening of area near the crack - Formation of small unstable panels located between successive cracks - Rupture of the structure 	<ul style="list-style-type: none"> - Weakening of area near the crack - Formation of small unstable panels located between successive cracks - Rupture of the structure 	<ul style="list-style-type: none"> - Weakening of area near the crack, then the arch; - Increased crack width; - Appearance of new cracks; - Falling blocks

Principally, the horizontal crack distribution is mainly attributed to transverse tunnel deformation within a ring subject to surrounding earth pressure. Figure 5 shows that fewer horizontal cracks develop in the area within 3 times the VCP diameter than those in the area from 3~5 times the VCP diameter. It is possibly due to the higher structural stiffnesses in the vicinity of the VCP compared to the areas farther away.

Likewise, similar crack distribution is also found for diagonal and vertical major long cracks. The fewer cracks near the VCP might indicate a strengthened design near VCP. Moreover, the direction of most diagonal cracks develops from the crown section of near - VCP side to the invert section of far - VCP side, which confirms with the twin tunnel effect revealed by Wang et al. (2023). That is, the twin tunnels move closer towards the centerline with slight tunnel settlement. Further study will specifically investigate the cross passage structural features, ground condition, VCP effect and etc.

In practice, the major engineering problems at a tunnel are highly related to water ingress (BOULOGNE et al. 2015). In DPT, water leakage is widely observed all along the tunnel length, with more on the crown section than other areas. That's because of the tension cracks on the crown and compaction on the sidewall. Along the tunnel length, the maintenance report indicates that the northern part shows more hydraulic deterioration. This may be due to high water pressure and its huge variation over time. The hydrogeological condition varies with seasonal and is also site-specific, as precipitation in Ireland is at extremes in winter and summer, which deserves further investigation in greater depth.

In summary, orthomosaics reveal that significant horizontal and diagonal cracks, as well as leakages, indicate improved structural stiffness within a distance of three times the VCP length, compared to areas located three to five times beyond these boundaries. This suggests the possibility of a more secure structural design and/or enhanced waterproofing in the VCP area. Conversely, the tunnel crown shows signs of worsened water ingress due to long-term deformation resulting from compression.

5. CONCLUSIONS

This paper applies a visual UAV navigation method for the automatic inspection of complex underground structures that does not rely on GNSS signals, additional sensors, or computer vision for navigation. The proposed method can automatically adapt the UAV navigation strategy for various tunnel diameters and geometries. The gathered image data are used to create a 3D reconstruction of the inspected tunnel section for structural condition assessment, which reveals the defects related to water ingress and structural compressive deformation.

ACKNOWLEDGEMENT

Ran Zhang acknowledges the support from the China Scholarship Council.

REFERENCES

- BOULOGNE, C. et al. 2015. Road tunnel civil engineering inspection guide Book 2: Catalogue of deteriorations. Available at: https://www.cetu.developpement-durable.gouv.fr/IMG/pdf/catalogue_of_deteriorations.pdf [Accessed: 4 June 2023].
- Jiménez-Jiménez, S.I., Ojeda-Bustamante, W., Marcial-Pablo, M. de J. and Enciso, J. 2021. Digital Terrain Models Generated with Low-Cost UAV Photogrammetry: Methodology and Accuracy. *ISPRS International Journal of Geo-Information* 10(5), p. 285. doi: 10.3390/ijgi10050285.
- Montero, R., Victores, J.G., Martínez, S., Jardón, A. and Balaguer, C. 2015. Past, present and future of robotic tunnel inspection. *Automation in Construction* 59, pp. 99–112. doi: 10.1016/j.autcon.2015.02.003.
- Tan, C.H. et al. 2018. A smart unmanned aerial vehicle (UAV) based imaging system for inspection of deep hazardous tunnels. *Water Practice and Technology* 13(4), pp. 991–1000. doi: 10.2166/wpt.2018.105.
- Wang, C., Friedman, M. and Li, Z. 2023. Monitoring and assessment of a cross-passage twin tunnel long-term performance using Wireless Sensor Network. *Canadian Geotechnical Journal*. Available at: <https://cdnsiencepub.com/doi/abs/10.1139/cgj-2022-0224> [Accessed: 29 May 2023].